Microscopic universality in the spectrum of the lattice Dirac operator

M.E. Berbenni-Bitsch¹, S. Meyer¹, A. Schäfer², J.J.M. Verbaarschot³, and T. Wettig^{4,5}

¹Fachbereich Physik – Theoretische Physik, Universität Kaiserslautern, D-67663 Kaiserslautern, Germany

²Institut für Theoretische Physik, Universität Regensburg, D-93040 Regensburg, Germany

³Department of Physics, State University of New York, Stony Brook, NY 11794, USA

⁴Max-Planck-Institut für Kernphysik, Postfach 103980, D-69029 Heidelberg, Germany

⁵Institut für Theoretische Physik, Technische Universität München, D-85747 Garching, Germany

(December 2, 1997)

Large ensembles of complete spectra of the Euclidean Dirac operator for staggered fermions are calculated for SU(2) lattice gauge theory. The accumulation of eigenvalues near zero is analyzed as a signal of chiral symmetry breaking and compared with parameter-free predictions from chiral random matrix theory. Excellent agreement for the distribution of the smallest eigenvalue and the microscopic spectral density is found. This provides direct evidence for the conjecture that these quantities are universal functions.

PACS numbers: 11.15.Ha, 05.45.+b, 11.30.Rd, 12.38.Gc

Hadronic properties such as the lightness of the pion masses and the absence of parity doublets, strongly indicate that chiral symmetry is broken spontaneously. In QCD, a great deal of insight in such nonperturbative phenomena has been obtained from extensive lattice QCD simulations [1,2]. This did not go without a significant amount of effort. One of the difficulties is that the order parameter of the chiral phase transition, $\langle \psi \psi \rangle$, can be obtained only after a complicated limiting procedure: the thermodynamic limit, the chiral limit, and the continuum limit. In addition, in the chiral limit it is extremely costly to take into account the effect of the fermion determinant. Since the fermion determinant can be expressed as a product over the Dirac eigenvalues, this alone warrants a detailed study of the QCD Dirac spectrum. Moreover, $\langle \bar{\psi}\psi \rangle$ is directly related to the QCD Dirac spectrum through the Banks-Casher relation [3],

$$\langle \bar{\psi}\psi \rangle = \lim_{m \to 0} \lim_{V \to \infty} \frac{\pi}{V} \rho(0).$$
 (1)

Here, m is the quark mass, V is the volume of space-time, and $\rho(\lambda) = \langle \sum_n \delta(\lambda - \lambda_n) \rangle$ is the eigenvalue density of the Euclidean Dirac operator, $iD = i\gamma_\mu \partial_\mu + \gamma_\mu A_\mu$, averaged over gauge field configurations. We observe that the average position of the smallest eigenvalues is determined by the chiral condensate. In this letter we focus on fluctuations of the smallest eigenvalues about their average position. It should be clear that such fluctuations affect the fermion determinant and are important for the understanding of finite size effects [4]. The hope is that they are given by universal functions which can be obtained analytically. This analytical information could then be used to facilitate extrapolations to the thermodynamic and chiral limits.

A similar situation arises in mesoscopic physics [5]. In these studies, it was shown that for a sufficient amount of disorder, spectral correlations are universal and can be obtained from a Random Matrix Theory (RMT) with only the basic symmetries included. On the other hand, the average spectral density is non-universal and requires specific knowledge of the dynamics of the system. In this letter we investigate the question whether a similar separation of scales takes place in QCD. Does the disorder of lattice QCD gauge field configurations result in universal fluctuations of the small Dirac eigenvalues?

According to the Banks-Casher relation, the low-lying Dirac eigenvalues are spaced as 1/V for $\langle \bar{\psi}\psi \rangle \neq 0$. Recent work by Leutwyler and Smilga [6] shows that this part of the spectrum is related to the pattern of chiral symmetry breaking by means of a class of sum rules for the inverse Dirac eigenvalues. It is natural to magnify the spectrum near $\lambda = 0$ by a factor of V. This leads to the introduction of the microscopic spectral density [7] defined by

$$\rho_s(z) = \lim_{V \to \infty} \frac{1}{V\Sigma} \rho\left(\frac{z}{V\Sigma}\right) , \qquad (2)$$

where Σ is the absolute value of $\langle \bar{\psi}\psi \rangle$. Based on the analysis of the Leutwyler-Smilga sum rules, it was conjectured [7] that this distribution is universal and only determined by the global symmetries of the QCD partition function, the number of flavors, and the topological charge. If that is the case it can be obtained from a much simpler theory with only the global symmetries as input. Such a theory is chiral RMT which will be discussed below. Whether or not QCD is in this universality class is a dynamical question that can only be answered by lattice QCD simulations. The investigation of this question is the main purpose of this letter. At this moment it can only be addressed on relatively small lattices where our results are consistent with zero topological charge. The pertinent question of what happens in the continuum limit has to be postponed to future work. In this limit we expect zero modes to become important. $\rho_s(z)$ is then different in different sectors of topological charge. However, on present day lattices with staggered fermions there seems to be no evidence of a "zero-mode zone" [8],

and the situation is controversial at best.

There are already several pieces of evidence supporting the conjecture that ρ_s is universal: (1) The moments of ρ_s generate the Leutwyler-Smilga sum rules [9]. (2) ρ_s is insensitive to the probability distribution of the random matrix [10,11]. (3) Lattice data for the valence quark mass dependence of the chiral condensate could be understood using the analytical expression for ρ_s [12,13]. (4) The functional form of ρ_s does not change at finite temperature [14]. (5) The analytical result for ρ_s is found in the Hofstadter model for universal conductance fluctuations [15]. (6) For an instanton liquid ρ_s shows good agreement with the random-matrix result [16]. However, a direct demonstration for lattice QCD was missing.

An analysis of Dirac spectra on the lattice was performed in Ref. [17] where it was shown that the spectral fluctuations in the bulk of the spectrum on the scale of the mean level spacing are universal and described by RMT. This showed that the eigenvalues of the Dirac operator are strongly correlated. Only few configurations were available in this study, but spectral ergodicity allowed to replace the ensemble average by a spectral average. However, spectral averaging is not possible for ρ_s since only the first few eigenvalues contribute. Therefore, a large number of configurations is essential.

We briefly summarize the main ingredients of chiral RMT. In a random-matrix model, the matrix elements of the operator under consideration are replaced by the elements of a random matrix with suitable symmetry properties. Here, the operator is the Euclidean Dirac operator iD which is hermitian. Because γ_5 anti-commutes with iD the eigenvalues occur in pairs $\pm \lambda$. In a chiral basis, the random-matrix model has the structure [7]

$$iD+im
ightarrow \left[egin{array}{cc} im & W \\ W^\dagger & im \end{array}
ight] \, ,$$

where W is a matrix whose entries are independently distributed random numbers. In full QCD with N_f flavors, the weight function used in averaging contains the gluonic action in the form $\exp(-S_{\rm gl})$ and N_f fermion determinants. In RMT, the gluonic part of the weight function is replaced by a Gaussian distribution of the random matrix W. The symmetries of W are determined by the anti-unitary symmetries of the Dirac operator. Depending on the number of colors and the representation of the fermions the matrix W can be real, complex, or quaternion real [18]. The corresponding random-matrix ensembles are called chiral Gaussian orthogonal (chGOE), unitary (chGUE), and symplectic (chGSE) ensemble, respectively. The microscopic spectral density has been computed analytically for all three ensembles [9,19,20].

We have performed numerical simulations of lattice QCD with staggered fermions and gauge group SU(2) for couplings $\beta=4/g^2=2.0, 2.2,$ and 2.4 on lattices of size $V=L^4$ with L=8, 10, and 16. This range of lattice parameters covers the crossover region from strong

to weak coupling of SU(2) [21]. The boundary conditions are periodic for the gauge fields and periodic in space and anti-periodic in Euclidean time for the fermions. In this work, we only study the quenched approximation using a hybrid Monte Carlo algorithm [22]. This made it possible to generate a large number of independent configurations (indicated in the figures). The analysis of unquenched data with 4 dynamical flavors is in progress.

In SU(2) with staggered fermions, every eigenvalue of iD is twofold degenerate due to a global charge conjugation symmetry. In addition, the squared Dirac operator $-D^2$ couples only even to even and odd to odd lattice sites, respectively. Thus, $-D^2$ has V/2 distinct eigenvalues. We use the Cullum-Willoughby version of the Lanczos algorithm [23] to compute the complete eigenvalue spectrum of the sparse hermitian matrix $-D^2$ in order to avoid numerical uncertainties for the low-lying eigenvalues. There exists an analytical sum rule, $tr(-D^2) = 4V$, for the distinct eigenvalues of $-D^2$ [24]. We have checked that this sum rule is satisfied by our data, the largest relative deviation was $\sim 10^{-8}$. We have also made a detailed study to determine the optimal acceptance rates and trajectory lengths [25]. The integrated autocorrelation times are in the range of 1 to 4. The chiral condensate was obtained by fitting the spectral density and extracting $\rho(0)$ and is given in Table I below.

The overall spectral density of the Dirac operator cannot be obtained in a random-matrix model since it is not a universal function. The lattice result for $\rho(\lambda)$ is displayed in Fig. 1 for $\beta=2.0,\ V=10^4$ and $\beta=2.4,\ V=16^4$, respectively. Note the strong decrease in $\langle\bar{\psi}\psi\rangle$ (in lattice units) for $\beta=2.4$, cf. Eq. (1) and Table I.

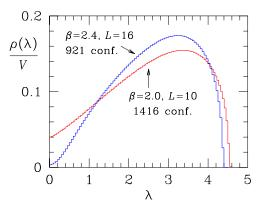


FIG. 1. Spectral density of the lattice Dirac operator for $\beta=2.0$ and 2.4. Only positive eigenvalues are plotted.

We are particularly interested in the region of small eigenvalues to check the predictions from chiral RMT. According to Ref. [18], staggered fermions in SU(2) have the symmetries of the chGSE. Analytical expressions can be obtained in the framework of RMT for the microscopic spectral density and the distribution of the smallest eigenvalue by slight modifications of results computed

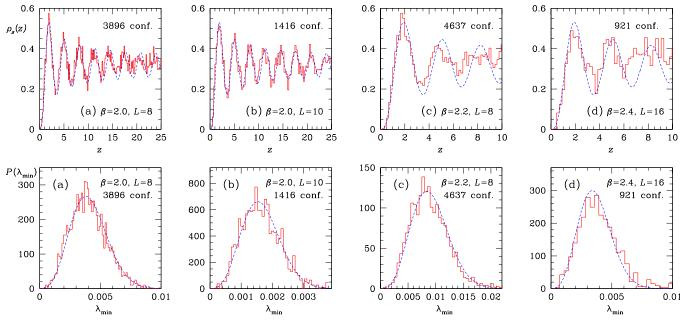


FIG. 2. Microscopic spectral density (upper row) and distribution of the smallest eigenvalue of the Dirac operator for different lattice parameters. From left to right the values of β are: 2.0, 2.0, 2.2, and 2.4. The histograms represent lattice data, the dashed curves are predictions from chiral RMT with $N_f = \nu = 0$.

for Laguerre symplectic ensembles [20,26]. Incorporating the chiral structure of the Dirac operator, we obtain from Ref. [20]

$$\rho_s(z) = 2z^2 \int_0^1 du u^2 \int_0^1 dv [J_{4a-1}(2uvz)J_{4a}(2uz) -vJ_{4a-1}(2uz)J_{4a}(2uvz)]$$
(3)

with $4a=N_f+2\nu+1$, where N_f is the number of massless flavors and ν is the topological charge. For our quenched data, 4a=1 since $\nu=0$ as explained in the introduction. According to Eq. (2), lattice data for $\rho_s(z)$ are constructed from the numerical eigenvalue density using a scale $V\langle\bar{\psi}\psi\rangle$. This scale is determined by the data, hence the random-matrix predictions are parameter-free. Similarly, the distribution of the smallest eigenvalue for $N_f=\nu=0$ follows from Ref. [26],

$$P(\lambda_{\min}) = \sqrt{\frac{\pi}{2}} c(c\lambda_{\min})^{3/2} I_{3/2}(c\lambda_{\min}) e^{-\frac{1}{2}(c\lambda_{\min})^2} , \quad (4)$$

where $c = V \langle \bar{\psi} \psi \rangle$ is the same scale as above. In Fig. 2 we have plotted the lattice results for $\rho_s(z)$ and $P(\lambda_{\min})$ together with the analytical results of Eqs. (3) and (4) for four different combinations of β and lattice size. The agreement between lattice data and the parameter-free RMT predictions is impressive. Note that the RMT results were derived in the limit $V \to \infty$. Clearly, the agreement improves as the physical volume increases, i.e., with larger lattice size and smaller β . From the results for $\beta = 2.0$ we observe that the agreement with RMT improves with increasing lattice size while the value of

condensate remains the same. This suggests that a similar improvement will occur for $\beta=2.2$ and $\beta=2.4$. These values are just below the β -value above which $\langle\bar{\psi}\psi\rangle$ approaches zero, where the above RMT results are inapplicable, and an increased sensitivity to the size of the lattice is expected. Since $P(\lambda_{\min})$ for these couplings agrees with the RMT distribution for zero topological charge we expect that the discrepancy for $\rho_s(z)$ is not due to a superposition of configurations with different topological charge. We hope that future work will clarify this issue.

Related quantities testing similar properties are the higher-order spectral correlation functions, in particular the two-point function which enters in the computation of scalar susceptibilities. The *n*-point correlation function $R_n(x_1,\ldots,x_n)$ is defined as the probability density of finding a level (regardless of labeling) around each of the points x_1, \ldots, x_n . The two-level cluster function $T_2(x,y)$, which contains only the non-trivial correlations, is defined by $T_2(x, y) = -R_2(x, y) + R_1(x)R_1(y)$, i.e., the disconnected part is subtracted. For the chGUE, there are analytical arguments [27] that the microscopic correlations are universal, and the same is expected for the chGSE. In this case, the predictions from RMT can again be obtained from the results of Ref. [20], but we do not write down the explicit expressions here. In Fig. 3, we have plotted data for $\rho_s(x,y)$ for $\beta=2.0$ on an 8^4 lattice as a function of x for some fixed value of y, along with the analytical random-matrix prediction. Clearly, the statistics are not as good as for the one-point function, but the agreement is still quite impressive.

Finally, we have checked the Leutwyler-Smilga sum

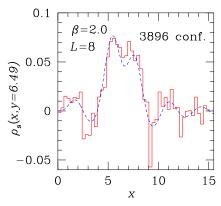


FIG. 3. Microscopic limit of the two-level cluster function for some fixed value of y. The histogram represents data for $\beta=2.0$ on an 8^4 lattice, the dashed curve shows the random-matrix prediction.

rule $\langle \sum_n \lambda_n^{-2} \rangle / V^2 = \langle \bar{\psi} \psi \rangle^2 / 2$ appropriate for the chGSE [6,28]. The numerical results are compared with the analytical predictions in Table I. Again, the agreement improves with physical volume.

TABLE I. Chiral condensate and a comparison of lattice data and analytical predictions for the Leutwyler-Smilga sum rule for λ_n^{-2} .

β	L	$\langle ar{\psi}\psi angle$	$\langle \sum_n \lambda_n^{-2} \rangle / V^2$	$\langle \bar{\psi}\psi \rangle^2/2$
2.0	8	0.1228(25)	$8.20(20)\cdot 10^{-3}$	$7.54(31) \cdot 10^{-3}$
2.0	10	0.1247(22)	$7.97(30) \cdot 10^{-3}$	$7.78(27) \cdot 10^{-3}$
2.2	8	0.0556(19)	$1.67(03) \cdot 10^{-3}$	$1.55(11) \cdot 10^{-3}$
2.4	16	0.00863(48)	$3.97(14) \cdot 10^{-5}$	$3.72(42)\cdot 10^{-5}$

In summary, we have performed a high-statistics study of the eigenvalue spectrum of the lattice QCD Dirac operator with particular emphasis on the low-lying eigenvalues. In the absence of a formal proof, our results provide very strong and direct evidence for the universality of ρ_s . In the strong coupling domain, the agreement with analytical predictions from random matrix theory is very good. On the scale of the smallest eigenvalues, agreement is found even in the weak-coupling regime. Furthermore, we found that the microscopic two-level cluster function agrees nicely with random-matrix predictions and that the Leutwyler-Smilga sum rule for λ_n^{-2} is satisfied more accurately with increasing physical volume. We predict that corresponding lattice data for SU(2)with Wilson fermions and for SU(3) with staggered and Wilson fermions will be described by random matrix results for the GOE, chGUE, and GUE, respectively [18]. (The U_A(1) symmetry is absent for the Hermitean Wilson Dirac operator.) The identification of universal features in lattice data is both of conceptual interest and of practical use. In particular, the availability of analytical results allows for reliable extrapolations to the chiral and thermodynamic limits. In future work we hope to analyze the fate of the fermionic zero modes in the approach to the continuum limit, and we expect random-matrix results to be a useful tool in the analysis.

It is a pleasure to thank T. Guhr and H.A. Weidenmüller for stimulating discussions. This work was supported in part by DFG and BMBF. SM and AS thank the MPI für Kernphysik, Heidelberg, for hospitality and support. The numerical simulations were performed on a CRAY T90 at the Forschungszentrum Jülich and on a CRAY T3E at the HWW Stuttgart.

- C. DeTar, Quark-gluon plasma in numerical simulations of QCD, in Quark gluon plasma 2, R. Hwa (ed.), World Scientific (Singapore) 1995.
- [2] A. Ukawa, Nucl. Phys. B (Proc. Suppl.) 53, 106 (1997).
- [3] T. Banks and A. Casher, Nucl. Phys. B **169**, 103 (1980).
- [4] M. Göckeler et al., Nucl. Phys. B 334, 527 (1990).
- [5] T. Guhr, A. Müller-Groeling, and H.A. Weidenmüller, cond-mat/9707301, to appear in Phys. Rep.
- [6] H. Leutwyler and A.V. Smilga, Phys. Rev. D 46, 5607 (1992).
- [7] E.V. Shuryak and J.J.M. Verbaarschot, Nucl. Phys. A 560, 306 (1993).
- [8] J.B. Kogut, J.F. Lagae, and D.K. Sinclair, hep-lat/9709067; A.L. Kaehler, hep-lat/9709141.
- [9] J.J.M. Verbaarschot and I. Zahed, Phys. Rev. Lett. 70, 3852 (1993).
- [10] E. Brézin, S. Hikami, and A. Zee, Nucl. Phys. B 464, 411 (1996).
- [11] S. Nishigaki, Phys. Lett. B 387, 139 (1996); G. Akemann et al., Nucl. Phys. B 487, 721 (1997).
- [12] S. Chandrasekharan and N. Christ, Nucl. Phys. B (Proc. Suppl.) 47, 527 (1996).
- [13] J.J.M. Verbaarschot, Phys. Lett. B 368, 137 (1996).
- [14] A.D. Jackson, M.K. Şener, and J.J.M. Verbaarschot, Nucl. Phys. B 479, 707 (1996).
- [15] K. Slevin and T. Nagao, Phys. Rev. Lett. 70, 635 (1993).
- [16] J.J.M. Verbaarschot, Nucl. Phys. B 427, 534 (1994).
- [17] M.A. Halasz and J.J.M. Verbaarschot, Phys. Rev. Lett. 74, 3920 (1995).
- [18] J.J.M. Verbaarschot, Phys. Rev. Lett. 72, 2531 (1994).
- [19] J.J.M. Verbaarschot, Nucl. Phys. B 426, 559 (1994).
- [20] T. Nagao and P.J. Forrester, Nucl. Phys. B 435, 401 (1995).
- [21] M. Creutz, Phys. Rev. D 21, 2308 (1980).
- [22] S. Duane et al., Phys. Lett. B 195, 216 (1987); S. Meyer and B. Pendleton, Phys. Lett. B 241, 397 (1990).
- [23] J. Stoer and R. Bulirsch, Introduction to Numerical Analysis, Springer (New York) 1993, § 6.5.3.
- [24] T. Kalkreuter, Phys. Rev. D 51, 1305 (1995).
- [25] M.E. Berbenni-Bitsch et al., Nucl. Phys. B (Proc. Suppl.) 53, 965 (1997).
- [26] P.J. Forrester, Nucl. Phys. B 402, 709 (1993).
- [27] T. Guhr and T. Wettig, hep-th/9704055; A.D. Jackson, M.K. Şener, and J.J.M. Verbaarschot, hep-th/9704056.
- [28] J.J.M. Verbaarschot, Phys. Lett. B **329**, 351 (1994).